JACS
JOURNAL OF THE AMERICAN CHEMICAL SOCIETY

Communication

pubs.acs.org/JACS

Effects of Microcomplexity on Hydrophobic Hydration in Amphiphiles

Ming-Liang Tan,[†] Joseph R. Cendagorta,[†] and Toshiko Ichiye*[,†,‡]

[†]Department of Chemistry, Georgetown University, Washington, D.C. 20057, United States

[‡]Laboratory of Computational Biology, National Heart, Lung and Blood Institute, National Institutes of Health, Bethesda, Maryland 20892, United States

Supporting Information

ABSTRACT: Hydrophobic hydration is critical in biology as well as many industrial processes. Here, computer simulations of ethanol/water mixtures show that a three-stage mechanism of dehydration of ethanol explains the anomalous concentration dependence of the thermodynamic partial molar volumes, as well as recent data from neutron diffraction and Raman scattering. Moreover, the simulations show that the breakdown of hydrophobic hydration shells, whose structure is determined by the unique molecular properties of water, is caused by the microcomplexity of the environment and may be representative of early events in protein folding and structure stabilization in aqueous solutions.

The changes in solvation of hydrophobic molecules upon association are the basis for the hydrophobic effect, found in protein folding[1] and formation of micelles and membranes.[2] However, since experimentally probing the water structure around dissociated hydrophobic molecules is difficult due to their low solubility, much of our current molecular view comes from computational and theoretical studies.[3,4] Although an iceberg-like hydration shell was proposed based on the anomalous concentration dependence of the partial molar volumes of alcohols in water,[5] the current view of the hydrophobic effect emphasizes a length-scale crossover at ∼1 nm.[3] Recently, neutron diffraction studies of methanol/water mixtures have shown molecular-level segregation consistent with hydrophobic effects, but no enhancement of water structure around nonpolar groups.[6,7] On the other hand, new Raman scattering measurements of *n*-alcohols have found hydrophobic hydration shells with greater tetrahedral order than in bulk water.[8] In addition, recent large-scale simulations of *t*-butanol/water mixtures have shown unphysical demixing at higher concentrations,[9] leading to concerns about the current water models. Here, extensive molecular dynamics simulations of ethanol/water mixtures reconcile these seemingly conflicting reports. A critical factor is the tetrahedral order of the hydrophobic hydration shell, which is determined by the unique properties of a water molecule but influenced by the microcomplexity of the environment. Moreover, the progressive breakdown of this shell with increasing ethanol concentration leads to a microcomplexity-driven model for hydrophobic association, which has implications for more complex molecules in aqueous solution.

Computer simulations of anomalous properties of liquid water can identify fundamental characteristics of a water molecule. For instance, a large molecular quadrupole appears essential for reproducing pure-liquid properties,[10] including the temperature of maximum density associated with hydrophobic solvation.[11] Of the models used here, SSDQO1[12,13] and TIP4P-Ew[14] have large quadrupole moments and a similar tetrahedral arrangement of two hydrogen bond donors and two acceptors (i.e., the coordination numbers n_{OwOw} are 4.39 and 4.48, respectively, and the Debenedetti measure of tetrahedrality q[15] are 0.671 and 0.658, respectively), while TIP3P[16] (as modified in the CHARMM force field[17]) has a small quadrupole and much more disordered donors (Figure 1). However, SSDQO1

Figure 1. Three-dimensional distribution of water around a water molecule (red and white stick) in the pure liquid, with red surface indicating probability density greater than 3 for TIP3P, TIP4P-Ew, and SSDQO1 (from left to right).

also accounts for the out-of-plane p-orbital electron density ("lone-pairs"), seen in quantum chemical calculations.[18] Thus, SSDQO1 has an *energetic* preference for tetrahedrality, while TIP4P-Ew relies on liquid-state packing to localize the donors.

While an energetic versus packing preference for tetrahedral order gives rise to similar structures for the pure liquid, the structure of the molecular hydration shell of the amphiphilic molecule ethanol at infinite dilution shows that it is not the case in solution (Figure 2). The *energetic* preference for the tetrahedral arrangement in SSDQO1 leads to a densely packed hydration shell (11.3 waters around the methyl) with tetrahedral order (around the methyl, n_{OwOw} = 3.81, q = 0.615) around the hydrocarbon tail. The recent Raman spectroscopy data support these results, showing that the hydrogen bonding in the hydration shell of highly dilute ethanol is more tetrahedral compared to bulk water at

Received: December 21, 2012
Published: March 18, 2013

   dx.doi.org/10.1021/ja312504q | *J. Am. Chem. Soc.* 2013, 135, 4918−4921

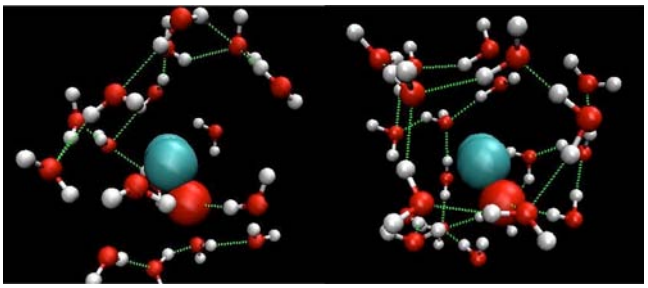

Figure 2. The ethanol hydration shell from simulations with TIP4P-Ew (left) and SSDQO1 (right). Large spheres are ethanol oxygens (red) and carbons (aqua); small spheres are water oxygens (red) and hydrogens (white).

moderate temperatures.[8,19] In contrast, the hydration shell is more stretched and distorted in TIP4P-Ew (even more so in TIP3P) since pure liquid packing no longer occurs. Even though the measures of tetrahedral order are only slightly different for first shell water (around the methyl, $n_{OwOw} = 3.90$, $q = 0.607$), the slightly greater number of waters allowed as neighbors disrupts the tetrahedrality enough so that there are fewer waters in the first shell (10.8 waters around the methyl). In addition, although ethanol/water interactions may play a role,[9] they were identical for TIP3P and SSDQO1 results shown and similar results were obtained with other ethanol parameters (see Supporting Information).

The behavior of the mixtures as a function of the mole fraction of ethanol (X_E) can be divided into three regions representing three distinct states in the dehydration of ethanol (Figure 3). In region I ($X_E < \sim 0.05$), the amount of bulk water (dark blue) decreases while the number of hydration shells (light blue) of ethanol increase and even come into contact (Figure 3, top left). Bulk water disappears at $X_E = \sim 0.05$, which corresponds to just enough water for about one hydration shell around each ethanol, although ~50% of the ethanol form dimers while the rest remain as monomers. Thus, in region II ($\sim 0.05 < X_E < \sim 0.25$), the hydration shells begin to break up into clusters of water (Figure 3, top right). Specifically, the (light blue) water around the hydrocarbon tails decreases while the (lime) water hydrogen-bonded to the ethanol hydroxyls remains, so that the tails begin to associate (Figure 3, bottom left). Essentially, only water hydrogen-bonded to the ethanol hydroxyls remains at $X_E = \sim 0.25$, which corresponds to maximum possible number of three water molecules hydrogen bonding to each ethanol hydroxyl group. Thus, in region III ($X_E > \sim 0.25$), the (lime) water bound to the ethanol hydroxyls decreases (Figure 3, bottom right).

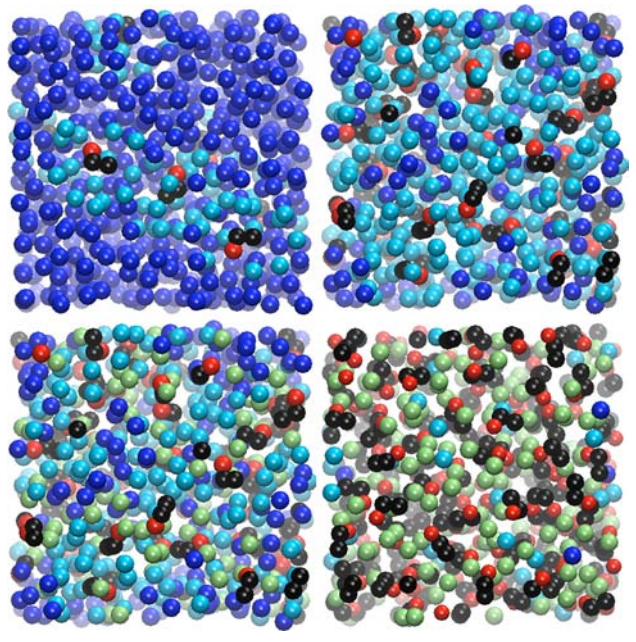

Figure 3. Ethanol/SSDQO1 mixtures from simulations in regions I ($X_E = 0.01$, top left), II ($X_E = 0.1$, top right and bottom left), and III ($X_E = 0.4$, bottom right). In the top figures, spheres represent water in ethanol hydration shells (light blue) and bulk (dark blue), while in the bottom figures, the hydration is divided into hydrophilic (lime) and hydrophobic (light blue). Also, spheres represent ethanol hydroxyls (red) and carbon (black) in all figures.

The coordination numbers show how the compositions of the molecular environments change as a function of X_E and can be compared to neutron diffraction studies[20] (Figure 4). Here,

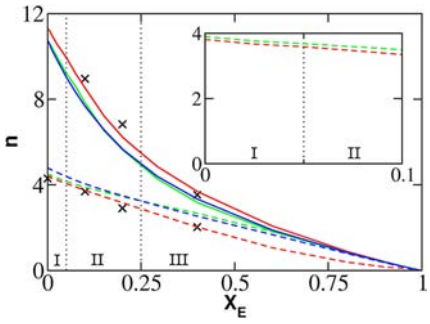

Figure 4. The coordination numbers n_{C2Ow} (solid) and n_{OwOw} (dashed) as a function of X_E from TIP3P (blue), TIP4P-Ew (green), and SSDQO1 (red) simulations and neutron diffraction data (×). The dotted lines separate regions I, II, and III. Inset is n_{OwOw} for the first hydration shell of the methyl carbon.

n_{XY} is the coordination number around a central atom X of type Y atom (X,Y = O_w, the water oxygen, or C_2, the methyl carbon). The n_{C2Ow} shows a nonlinear decrease with increasing X_E, with a fast decrease in regions I and II due to the decreasing hydrophobic hydration and a slower decrease in region III due to the dehydration of the ethanol hydroxyl. However, n_{C2Ow} is consistently larger in SSDQO1 and experiment than TIP4P-Ew because of the larger number of waters in the tetrahedrally ordered hydrophobic hydration shell. In addition, the nonlinear decrease n_{OwOw} and large values of n_{C2Ow} seen in SSDQO1 and experiment indicate a preference for formation of hydration shells over water clusters. In contrast, the linear behavior of n_{OwOw} of TIPnP is consistent with the unphysical demixing seen in the 64 000 particle simulations of *t*-butanol in water at $X_E = 0.1$[9] since water clustering is favored.

In addition, the n_{OwOw} of just waters hydrating the C_2 show a change in region I compared to the 4.4 neighbors found in bulk (Figure 4, inset). At infinite dilution, this n_{OwOw} is 3.8, in agreement with the Raman data at $X_E < 0.01$, which indicates that the tetrahedrally ordered hydration shell waters also have fewer weak hydrogen bonds than bulk,[8] apparently due to the loss of the interstitial water.[21] As dimerization begins to occur, the water in hydration shells that come into contact must satisfy the tetrahedral constraints of each shell. This suggests the tetrahedral ordering is breaking down so that the water is becoming more bulk-like, which is supported by lack of

dx.doi.org/10.1021/ja312504q | *J. Am. Chem. Soc.* 2013, 135, 4918−4921

enhancement of the hydration shell water in the neutron diffraction studies of slightly more concentrated solutions (i.e., mole fraction of 0.05 for methanol[7]).

The concentration dependence of the partial molar volumes of ethanol V_E and water V_W are thermodynamic properties that are influenced by the changing molecular environments and can be compared to density measurements[22] (Figure 5). In the simulations, the decrease in $V_E(0)$ with respect to $V_E(1)$ appears to be proportional to the tetrahedral order of the bulk water (Figure 1), and the experimental decrease has been attributed to the compressive effects of water around hydrocarbons.[23,24] However, in SSDQO1, V_E actually decreases in region I from its infinite dilution value by ∼2 cc/mol to a minimum near X_E = ∼0.05, in agreement with experiment. Although this phenomenon is widely known, it has not been interpreted molecularly to our knowledge. Here, it is attributed to a decrease in the free volume around the tail as the hydration shells come into contact with other hydration shells, with the transition from enhanced tetrahedral order to greater more bulk-like disorder in the shell leading to tighter packing against the hydrocarbon. However, in the TIPnP models, the free volume change is minimized because the hydration shells are already distorted before they come into contact. In addition, the appearance of disordered hydration in the Raman data for *n*-alcohols of between four to seven carbons at high temperatures[8] is consistent with the changes in the partial molar volume behavior for the longer alcohols at high temperatures[25] rather than a length-scale crossover, which occurs at 20 carbons for *n*-alkanes.[3]

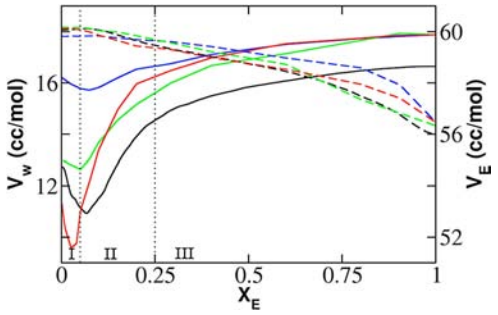

Figure 5. The partial molar volumes of ethanol, V_E (solid lines, right axis), and water, V_W (dashed, left axis), from TIP3P (blue), TIP4P-Ew (green), and SSDQO1 (red) simulations and density data (black). The dotted lines separate regions I, II, and III.

Further increasing X_E leads to a sharp increase in V_E (region II) as the hydration shells break down and the ethanol tails coalesce (Figure 3, X_E = 0.1). Here, the loose packing of hydrocarbon against hydrocarbon increases the free volume around the ethanol. Also, for V_W, a slight expansion occurs near X_E = ∼0.05 and a subsequent decrease in region II occurs more noticeably in the SSDQO1 simulations, in agreement with experiment. While this has previously been attributed to a breakdown of liquid water structure,[26] the simulations suggest a more complete explanation. In particular, the slight increase is due to the increasing proportion of hydration shells to bulk, while the decrease is due to the decreasing proportion of the partially tetrahedral hydrophobic hydration shells to the remaining disordered hydrating water clusters and strings.

A second weaker transition occurs at X_E = ∼0.25 where methanol/water mixtures appear to change from a water-only percolating to a bipercolating mixture,[27] and other thermodynamic anomalies also appear.[23] V_E increases more slowly in region III, because the three hydrogen-bonding waters of the ethanol hydroxyl are replaced by two hydrogen-bonding ethanols, and the free volume is less affected.

The concentration dependent behavior shown here implies a mode of hydrophobic association for amphiphilic molecules in which the hydration changes as a result of the microcomplexity of the solute environment. In this model, hydrophobic moieties that are far apart have tetrahedrally ordered hydration shells that stabilize the separated species. As the hydration shells come into contact, the shells become partially disordered as the hydrating waters at the point of contact satisfy the constraints of both shells, but stay mostly intact so that the hydrophobic moieties remain solvated (region I). Next, the shells break apart as the concentration of hydrophobic moieties increases when the hydrating water can no longer satisfy the constraints imposed by the presence of multiple hydration shells (region II). Finally, the hydrophilic moieties become desolvated (region III).

The different stages in the desolvation processes identified in this study may also play a role in key events in protein folding, from the initial dehydration of the unfolded polypeptide[28] to the final expulsion of water that leads to the folded, stable protein in solution.[29] Moreover, the importance of microcomplexity is consistent with recent studies of the role of the chemical heterogeneity in hydrophobic protein surfaces[30] and the extensiveness of the changes in the structure of water in the binding of proteins and ligands.[31]

■ ASSOCIATED CONTENT

Supporting Information

Molecular simulation methods. This material is available free of charge via the Internet at http://pubs.acs.org.

■ AUTHOR INFORMATION

Corresponding Author

ti9@georgetown.edu

Notes

The authors declare no competing financial interest.

■ ACKNOWLEDGMENTS

We are grateful to the National Science Foundation (grant number CHE-1158267, T.I.) and to the McGowan Foundation (T.I.) for the support of this work. We also thank Benjamin T. Miller and Bernard R. Brooks for assistance in implementing the code, Peter J. Rossky and Sergio A. Hassan for insightful discussions, and Alan K. Soper for providing the neutron diffraction data for the aqueous solutions of methanol and ethanol.

■ REFERENCES

(1) Kauzmann, W. *Adv. Protein Chem.* **1959**, *14*, 1.
(2) Tanford, C. *The Hydrophobic Effect: Formation of Micelles and Biological Membranes*; Wiley: New York, 1973.
(3) Chandler, D. *Nature* **2005**, *437*, 640.
(4) Ashbaugh, H. S.; Pratt, L. R. *Rev. Mod. Phys.* **2006**, *78*, 159.
(5) Frank, H. S.; Evans, M. W. *J. Chem. Phys.* **1945**, *13*, 507.
(6) Dixit, S.; Crain, J.; Poon, W. C. K.; Finney, J. L.; Soper, A. K. *Nature* **2002**, *416*, 829.
(7) Dixit, S.; Soper, A. K.; Finney, J. L.; Crain, J. *Europhys. Lett.* **2002**, *59*, 377.
(8) Davis, J. G.; Gierszal, K. P.; Wang, P.; Ben-Amotz, D. *Nature* **2012**, *49*, 582.

(9) Gupta, R.; Patey, G. N. *J. Chem. Phys.* **2012**, *137*, 034509.
(10) Abascal, J. L. F.; Vega, C. *Phys. Rev. Lett.* **2007**, *98*, 237801.
(11) Paschek, D. *J. Chem. Phys.* **2004**, *120*, 6674.
(12) Ichiye, T.; Tan, M.-L. *J. Chem. Phys.* **2006**, *124*, 134504.
(13) Te, J. A.; Ichiye, T. *J. Chem. Phys.* **2010**, *132*, 114511.
(14) Horn, H. W.; Swope, W. C.; Pitera, J. W.; Madura, J. D.; Dick, T. J.; Hura, G. L.; Head-Gordon, T. *J. Chem. Phys.* **2004**, *120*, 9665.
(15) Errington, J. R.; Debenedetti, P. G. *Nature* **2001**, *409*, 318.
(16) Jorgensen, W. L.; Chandrasekhar, J.; Madura, J. D.; Impey, R. W.; Klein, M. L. *J. Chem. Phys.* **1983**, *79*, 926.
(17) MacKerell, A. D., Jr.; Bashford, D.; Bellot, M.; Dunbrack, R. L., Jr.; Field, M. J.; Fischer, S.; Gao, J.; Guo, H.; Ha, S.; Joseph, D.; Kuchnir, K.; Kuczera, K.; Lau, F. T. K.; Mattos, M.; Michnick, S.; Nguyen, D. T.; Ngo, T.; Prodhom, B.; Roux, B.; Schlenkrich, M.; Smith, J.; Stote, R.; Straub, J.; Wiorkiewicz-Kuczera, J.; Karplus, M. *J. Phys. Chem. B* **1998**, *102*, 3586.
(18) Niu, S.; Tan, M.-L.; Ichiye, T. *J. Chem. Phys.* **2011**, *134*, 134501.
(19) For simplicity, we consider that hydrogen bonds are formed between oxygens of either water or ethanol if they are within 3.3 Å of each other since the O−H radial distribution functions are consistent with the formation of hydrogen bonds, although there are more rigorous definitions.
(20) Soper, A. K. Personal communication.
(21) Rossky, P. J.; Zichi, D. A. *Faraday Symp. Chem. Soc.* **1982**, *17*, 69.
(22) Council, N. R. *International Critical Tables*; 1st ed.; Mc-Graw Hill: New York, 1926.
(23) Franks, F.; Ives, D. J. G. *Quart. Rev. Chem. Soc.* **1966**, *20*, 1.
(24) The overestimate of the decrease in $V_E(0)$ and the subsequent underestimate of the concentration of the minimum in SSDQO1 are due to a slight overestimate of the hydration of the ethanol hydroxyl and do not affect the conclusions.
(25) Nakanishi, K.; Kato, N.; Maruyama, M. *J. Phys. Chem.* **1967**, *71*, 814.
(26) Mitchell, A. G.; Wynne-Jones, W. F. K. *Discuss. Faraday Soc.* **1953**, *15*, 161.
(27) Dougan, L.; Bates, S. P.; Hargreaves, R.; Fox, J. P.; Crain, J.; Finney, J. L.; Réat, V.; Soper, A. K. *J. Chem. Phys.* **2004**, *121*, 6456.
(28) Matysiak, S.; Debenettti, P. G.; Rossky, P. J. *J. Phys. Chem. B* **2011**, *115*, 14859.
(29) Cheung, M. S.; García, A. E.; Onuchic, J. N. *Proc. Natl. Acad. Sci. U.S.A.* **2003**, *99*, 685.
(30) Giovambattista, N.; Lopez, C. F.; Rossky, P. J.; Debenedetti, P. G. *Proc. Natl. Acad. Sci. U.S.A.* **2008**, *105*, 2274.
(31) Snyder, P. W.; Mecinovic, J.; Moustakas, D. T.; Thomas, S. W., III; Harder, M.; Mack, E. T.; Lockett, M. R.; Héroux, A.; Sherman, W.; Whitesides, G. M. *Proc. Natl. Acad. Sci. U.S.A.* **2011**, *108*, 17889.